Physica A 503 (2018) 9–25

Contents lists available at ScienceDirect

Physica A

journal homepage: www.elsevier.com/locate/physa

Reservoir effects on the temperature dependence of the relaxation to equilibrium of three simple quantum systems

A.A. Ierides *, V.M. Kenkre

Department of Physics and Astronomy, University of New Mexico, Albuquerque, NM 87131, United States

HIGHLIGHTS

- Results include nonmonotonicity of relaxing observables, e.g. energy, when T is changed.
- The effect appears only under strong interactions and is directly observable in principle.
- Useful procedures developed: a half-Markoffian approximation and a relaxation memory/rate.

ARTICLE INFO

Article history:
Received 21 November 2017
Received in revised form 22 February 2018
Available online 1 March 2018

Keywords:
Approach to thermal equilibrium
Nonmonotonic temperature dependence
Multiphonon
Single-phonon
Vibrational relaxation
Polaronic transformation

ABSTRACT

The approach to thermal equilibrium of each of three simple quantum systems in interaction with a reservoir is analyzed by calculating the time evolution of an observable appropriate for each system. Two types of interaction with the reservoir are considered: a single-phonon modulation of the interaction matrix element and a multiphonon interaction arising from a polaronic transformation for a given single-phonon, but strong, modulation of energy or frequency. The methodology employed is a recent formalism based on a coarse-grained generalized master equation. Interesting results are obtained for the multiphonon case including a nonmonotonic dependence of the time-dependent observables in the multiphonon system as the temperature is varied. Such a result does not appear in the single-phonon case, *i.e.*, for weak coupling. In addition to contributing towards the understanding of the detail in the approach to thermal equilibrium, the analysis has *practical* applications to the vibrational relaxation of molecules embedded in phonon baths and to the transport of charge in crystals subjected to electric fields strong enough to lead to the formation of Stark ladders.

1. Introduction and tools of this theoretical investigation

The purpose of this paper is to analyze the process of the approach to equilibrium of three simple but typical quantum systems in interaction with a specified thermal reservoir and to describe interesting features that arise when the interaction is strong. Approach to equilibrium is one of the subjects universally considered central in statistical mechanics [1–5] and worthy of careful investigation. The three systems considered for analysis in the present paper are a nondegenerate quantum dimer [6] which can exist in one of two energetically inequivalent states, differing in energy by 2Δ; a charged particle under the action of an applied strong electric field [7–10] E, moving across a 1-dimensional crystal of lattice constant, a; and a harmonic oscillator of frequency Ω representing a molecule relaxing vibrationally [11,12] as a result of its interaction with the reservoir [13]. The reservoir is a set of bosons, for instance phonons, of average frequency ω_0 and dispersion σ. The

* Corresponding author.
E-mail addresses: aierides@unm.edu (A.A. Ierides), kenkre@unm.edu (V.M. Kenkre).

https://doi.org/10.1016/j.physa.2018.02.210
0378-4371/

dimensionless coupling constant g determines the strength of the interaction between system and reservoir and is taken to lie between 0.02 and 2, depending on the coupling strength regime being studied, as described below.

The time-dependent observables calculated in order to study the approach to equilibrium are, in the first case, the occupation probability difference $p(t) = P_1(t) - P_2(t)$ of the dimer states which, from an initial value of 1 at the start, settles into the Boltzmann ratio, $-\tanh(\beta\Delta)$, where (and henceforth) $\beta = 1/k_BT$ with k_B the Boltzmann constant and T the temperature; in the second case, the velocity $v(t)$ of the electric charge q, as it speeds in the direction of the applied field; and in the third case, the average energy of the relaxing molecule $E(t) = \hbar\Omega\,(\langle M\rangle + 1/2)$, where $\langle M\rangle$ is the average number of excitations in the oscillator. The parameters involved in all three cases are, in addition to the temperature T and the coupling constant g, the following: the dispersion of the bath phonons, $\sigma \ll \omega_0$, and the characteristic energy of each system, 2Δ for the dimer, $\mathcal{E} = qEa$ for the moving charge, and $\hbar\Omega$ for the harmonic oscillator.

The tools that we use for our theoretical investigation are based on generalized master equations (GMEs) derived by extending the methodology of Zwanzig [14–16] to include coarse-graining [10,17,18]. We refer the reader to Refs. [6,10,19] for the derivation of the form of these GMEs, but display them immediately below for use in our subsequent calculations in the present paper.

As stated above, each of the three systems is characterized by a single energy. It is the difference 2Δ between the two dimer state energies in the first system, and the difference between nearest neighboring states for the other systems, $\mathcal{E}$ for the second and $\hbar\Omega$ for the third. For all three systems, the reservoir contributes to the respective GME an energetically "downward" memory $\phi_-(t)$ and an "upward" memory $\phi_+(t)$, decided solely by the reservoir. The $t = 0$ to ∞ time integrals of these memories are in a detailed balance ratio to each other, $\int_0^\infty ds\,\phi_-(s)/\int_0^\infty ds\,\phi_+(s) = e^{\beta\hbar\Omega}$, the characteristic frequency of the specified system being represented by Ω.

For the dimer, the occupation probabilities $P_1(t)$ and $P_2(t)$ of the two states obey

$$\frac{dP_1(t)}{dt} = F_{21}\int_0^t ds\,\left[\phi_+(t-s)P_2(s) - \phi_-(t-s)P_1(s)\right], \tag{1a}$$

$$\frac{dP_2(t)}{dt} = F_{21}\int_0^t ds\,\left[\phi_-(t-s)P_1(s) - \phi_+(t-s)P_2(s)\right], \tag{1b}$$

where F_{21} is the relaxation rate corresponding to the energetically downward interstate transition. Here, 1 denotes the higher energetic state, and $F_{12}/F_{21} = \exp(-2\Delta/k_BT)$, satisfy the detailed balance condition. The dynamics of the charge under the influence of a strong electric field are governed by the GME

$$\begin{aligned}\frac{dP_M(t)}{dt} = {} & \varkappa\int_0^t ds\,\left[\phi_-(t-s)P_{M+1}(s) + \phi_+(t-s)P_{M-1}(s)\right] \\ & - \varkappa\int_0^t ds\,\left[\phi_-(t-s) + \phi_+(t-s)\right]P_M(s),\end{aligned} \tag{2}$$

where $\varkappa$ is the charged particle relaxation rate, similarly the transition rate in the direction of the external field.[1] For the relaxing molecule represented by a harmonic oscillator, the occupation probability of the oscillator state M is governed by the GME described by

$$\begin{aligned}\frac{dP_M(t)}{dt} = \kappa\int_0^t ds\,\Big\{ & \phi_-(t-s)\left[(M+1)P_{M+1}(s) - MP_M(s)\right] \\ & - \phi_+(t-s)\left[(M+1)P_M(s) - MP_{M-1}(s)\right]\Big\},\end{aligned} \tag{3}$$

where κ is the downward transition rate which we will call the oscillator relaxation rate. The level spectrum is discrete in all cases, being finite (spanning only two states) in the first, infinite in the second (M's are integers from $-\infty$ to ∞), and semi-infinite (M's are positive integers extending from 0 to ∞) in the third system, respectively.

The GMEs in Eqs. (1)–(3), although slightly different in form as a result of the characteristics of each system, all have in them memories $\phi_\pm(t)$ which are identical because we treat identical baths influencing the systems. The difference between the GMEs arises in the terms multiplying the $\phi(t)$'s due to the respective system properties. The multiplicative terms are the corresponding relaxation rates, F_{21} for the dimer, $\varkappa$ for the charged particle, and κ (as well as site-index dependent terms) for the harmonic oscillator.

The present paper is organized as follows. In Section 2, brief comments are made about the form of the interaction analyzed and bath correlation functions common for all three systems are calculated along with expressions for the memories $\phi_\pm(t)$. The discussion is presented in the detailed context of the third system, the relaxing molecule, and results are used for all three cases without repeating the detail. In the next three sections, the relevant observable for each system is analyzed and the results are discussed. Concluding remarks are presented in the last section.

[1] In writing Eq. (2) we have corrected a minor sign error in Ref. [10].

2. Choice of interaction, calculation of the bath correlation function, and the nonmonotonicity effect

The interaction of the vibrating molecule with the bath that led to the well-known Montroll–Shuler relaxation equation [11] in chemical physics [12,20–26] was based on Landau–Teller rates [13]. For the sake of simplicity these assumed the interaction to be linear in the molecule displacement. Little more had to be specified in such a derivation because rates in the incoherent Master equation was all that was required. Our present interest, however, lies in a more detailed description that is capable of describing stages of the approach to equilibrium that are *earlier in time* as well and can give rise to effects like oscillations that occur during decoherence of the initial state. The memory functions required for this purpose demand more information about the basic system–bath interaction. Therefore, while we maintain the linear dependence feature of the Landau–Teller rates, we specify details of the bath observables in the interaction. Two types of interaction appear to us to be of interest and relevance. Both are compatible with the earlier analysis in the literature [13]. One of them is associated with weak coupling and single-phonon transitions while the other is best described as arising from strong coupling with single phonons leading, after a transformation, to multiphonon transitions. Our primary focus is in the latter because of its interesting consequences. We specify the two interactions in the Hamiltonian below. We comment on the noteworthy features of the approach to equilibrium that arise in the strong, multiphonon interaction case and show how they do not arise in the other, weak, single-phonon case.

2.1. The interaction Hamiltonians

Although the formalism can be developed for a completely general Hamiltonian, we will consider here separable cases of the form [12,27]

$$\mathscr{H} = \mathcal{H}_S + \mathcal{H}_B + \sum_j \mathscr{V}_{S,j}\mathscr{V}_{B,j}, \tag{4}$$

where $\mathcal{H}_S$ is the system Hamiltonian and $\mathscr{V}_{S,j}$ is the jth system contribution to the system–bath interaction, respectively. Each of these is different for each of the three systems. On the other hand $\mathcal{H}_B$ and $\mathscr{V}_{B,j}$, the bath Hamiltonian and jth bath-contributed interaction, respectively, are considered identical for all of the three systems studied. In order to use the perturbative tools mentioned in Section 1, the third term in Eq. (4) has to be weak relative to the other terms. Weak interactions do satisfy the requirements of the situation that, as a result of them, the system must eventually settle in a Boltzmann-weighted and random-phased density matrix in the eigenstates of $\mathcal{H}_S$ and $\mathcal{H}_B$. However, interesting results, as we shall show in the sequel, only emerge when the interaction is strong. To resolve this conundrum, we will consider *strong* interactions, a part of which can be taken into account *exactly* through a transformation resulting in a counterpart of Eq. (4). The interactions left over after the transformation will be weak and amenable to a perturbative treatment. We will also compare, in each case, the results of the strong interaction with those of the original weak interaction that does not produce interesting results.

Let us define the operators

$$H_B = \sum_q \hbar\omega_q \left(b_q^\dagger b_q + \frac{1}{2}\right), \tag{5a}$$

$$V_B = \sum_q g_q \hbar\omega_q \left(b_q + b_q^\dagger\right), \tag{5b}$$

where the b_q's describe bath bosons, for instance phonons, of frequency ω_q and wavevector q and the g_q's are the dimensionless coupling constants determining the interaction strength. In the first instance, we take the unperturbed bath Hamiltonian $\mathcal{H}_B$ to equal H_B and assume a single bath contribution j in the interaction, $\mathscr{V}_{B,j} = V_B$, weak enough so that the calculational procedure can use a perturbation in orders of the third term of Eq. (4). The system operators for this first system, the vibrating molecule, are

$$\mathcal{H}_S = \hbar\Omega \left(a^\dagger a + \frac{1}{2}\right), \tag{6a}$$

$$\mathscr{V}_S = a + a^\dagger, \tag{6b}$$

where Ω is the oscillator frequency and $a + a^\dagger$ is essentially the displacement of the molecular oscillator.

In order to analyze strong coupling, we begin by considering, as our second case, the same $\mathcal{H}_S$ as in Eq. (6a) and the same $\mathcal{H}_B = H_B$ as in Eq. (5a), but $V_B a^\dagger a + u(a + a^\dagger)$ as the system–bath interaction. The c-number u which describes the constant force exerted by the bath on the molecular oscillator is weak but V_B in this case is not because the coupling constants g_q are taken to be large. The term proportional to V_B *cannot* be treated in this second case perturbatively. In order to take as much of its effects into account exactly, we perform the standard polaronic transformation [20–24,28] taking the Hamiltonian from a representation in terms of the bare operators a, b, to a representation in terms of their dressed versions A, B. The

transformation, as is well known [20–24,28], corresponds to a shift of the equilibrium position of the bath oscillators and allows the Hamiltonian to be written as

$$\mathscr{H} = \left(\hbar\Omega - \sum_q g_q^2\hbar\omega_q\right)A^\dagger A + \sum_q \hbar\omega_q\left(B_q^\dagger B_q + \frac{1}{2}\right) + u\left[Ae^{\sum_q g_q\left(B_q - B_q^\dagger\right)} + A^\dagger e^{-\sum_q g_q\left(B_q - B_q^\dagger\right)}\right]. \tag{7}$$

Here, the dressed operators A and B are given by $A = ae^{-\sum_q g_q\left(B_q - B_q^\dagger\right)}$ and $B_q = b_q + g_q a^\dagger a$. We see that Eq. (7) is precisely of the form of Eq. (4) with $\mathcal{H}_S = \left(\hbar\Omega - \sum_q g_q^2\hbar\omega_q\right)A^\dagger A$ and $\mathcal{H}_B = \sum_q \hbar\omega_q\left(B_q^\dagger B_q + 1/2\right)$. The interaction term in the second line of Eq. (7) is amenable to a perturbative treatment because of the assumed smallness of the c-number u. The presence of the so-called phonon clouds (the exponentials of the dressed bath operators B_q, $B_q^\dagger$) forces the transformed Hamiltonian of Eq. (7) to have a *multiphonon* nature although the original Hamiltonian before the transformation has only single-phonon interactions.

2.2. Bath correlation functions

The GMEs (1)–(3) that govern the evolution of the three systems can be unified in the form

$$\frac{dP_M(t)}{dt} = \sum_N \int_0^t ds\, [\mathscr{W}_{MN}(t-s)P_N(s) - \mathscr{W}_{NM}(t-s)P_M(s)] \tag{8}$$

where the M and N refer to the system states. Expressions for the $\mathcal{W}(t)$'s are available in previous work in terms of the system, M and N, and bath, m and n, states as

$$\mathcal{W}_{MN}(t) = \frac{2}{\hbar^2}\sum_{m,n}\frac{e^{-\beta\epsilon_n}}{\mathcal{Z}}|\langle M,m|\mathscr{V}|N,n\rangle|^2\cos\left[(\omega_{mn}+\Omega_{MN})t\right], \tag{9a}$$

$$\mathcal{W}_{NM}(t) = \frac{2}{\hbar^2}\sum_{m,n}\frac{e^{-\beta\epsilon_n}}{\mathcal{Z}}|\langle M,m|\mathscr{V}|N,n\rangle|^2\cos\left[(\omega_{mn}-\Omega_{MN})t\right]. \tag{9b}$$

found for instance in Eqs. (A.3) and (A.4) of Ref. [10]. The method to arrive at Eqs. (8) and (9) employs the Zwanzig projection technique [14–16] generalized via coarse-graining [10,17,18]. Here $\Omega_{MN} = (E_M - E_N)/\hbar$ and $\omega_{mn} = (\epsilon_m - \epsilon_n)/\hbar$ are the frequencies corresponding to the energy differences between the system and bath states, respectively, $\mathcal{Z} = \sum_n e^{-\beta\epsilon_n}$ is the bath partition function, and $\mathscr{V}$ is the system–bath interaction.

While $\mathscr{V}$ may be generally of arbitrary form, we have taken it here, as explained in the context of Eq. (4), as a sum of products of independently contributing bath and system components. Showing expressions only for a single j for simplicity, we see that

$$\mathcal{W}_{MN}(t) = \frac{1}{\hbar^2}|\langle M|\mathscr{V}_S|N\rangle|^2\sum_{m,n}\frac{e^{-\beta\epsilon_n}}{\mathcal{Z}}|\langle m|\mathscr{V}_B|n\rangle|^2\left[e^{i(\omega_{mn}+\Omega_{MN})t} + e^{-i(\omega_{mn}+\Omega_{MN})t}\right], \tag{10a}$$

$$\mathcal{W}_{NM}(t) = \frac{1}{\hbar^2}|\langle M|\mathscr{V}_S|N\rangle|^2\sum_{m,n}\frac{e^{-\beta\epsilon_n}}{\mathcal{Z}}|\langle m|\mathscr{V}_B|n\rangle|^2\left[e^{i(\omega_{mn}-\Omega_{MN})t} + e^{-i(\omega_{mn}-\Omega_{MN})t}\right]. \tag{10b}$$

Distributing the exponents in Eqs. (10) so that bath quantities are absorbed into factors separated from the system quantities, we obtain

$$\mathscr{W}_{MN}(t) = \frac{1}{\hbar^2}|\langle M|\mathscr{V}_S|N\rangle|^2\left[e^{i\Omega_{MN}t}\mathscr{B}(t) + e^{-i\Omega_{MN}t}\mathscr{B}^*(t)\right], \tag{11a}$$

$$\mathscr{W}_{NM}(t) = \frac{1}{\hbar^2}|\langle M|\mathscr{V}_S|N\rangle|^2\left[e^{-i\Omega_{MN}t}\mathscr{B}(t) + e^{i\Omega_{MN}t}\mathscr{B}^*(t)\right]. \tag{11b}$$

The fact that Eq. (11) presents the memories as a direct combination of, on one hand the system detail in the matrix elements of $\mathscr{V}_S$ and the difference Ω_{MN}, and on the other the bath correlation function $\mathscr{B}(t)$, a property entirely of the bath given by

$$\mathscr{B}(t) = \sum_{m,n}\frac{e^{-\beta\epsilon_n}}{\mathcal{Z}}\langle m|\mathscr{V}_B|n\rangle\langle n|\mathscr{V}_B^\dagger(t)|m\rangle = \frac{\mathrm{Tr}\left(e^{-\beta\mathcal{H}_B}\mathscr{V}_B e^{i\mathcal{H}_B t/\hbar}\mathscr{V}_B^\dagger e^{-i\mathcal{H}_B t/\hbar}\right)}{\mathrm{Tr}\left(e^{-\beta\mathcal{H}_B}\right)}, \tag{12}$$

is calculationally significant. It stems from the reasonable, normally made, supposition that the bath always remains in its thermal equilibrium even as it influences the time evolution of the system. For our three systems, M and N differ only by 1 such that only transitions between nearest neighbor states can occur. Their energy difference is $\pm\hbar\Omega$, depending on the respective transition direction, Ω being the system specific characteristic frequency.

Explicit calculation from Eq. (5) gives, for the weak-coupling case,

$$\mathscr{B}(t) = \sum_q g_q^2 \hbar^2 \omega_q^2 \left[\coth\left(\frac{\beta\hbar\omega_q}{2}\right) \cos\omega_q t + i \sin\omega_q t \right]. \tag{13}$$

The evaluation is more involved for the strong-coupling case of Eq. (7), but follows standard polaronic manipulations [20–24,28,29] and yields

$$\mathscr{B}(t) = u^2 e^{-\sum_q g_q^2 \coth\left(\frac{\beta\hbar\omega_q}{2}\right)} e^{\frac{1}{2}\sum_q g_q^2 \operatorname{csch}\left(\frac{\beta\hbar\omega_q}{2}\right)\left(e^{\frac{\beta\hbar\omega_q}{2}} e^{i\omega_q t} + e^{-\frac{\beta\hbar\omega_q}{2}} e^{-i\omega_q t}\right)}. \tag{14}$$

In order to perform the summation over the reservoir modes q implicit in $\mathscr{B}(t)$ in Eqs. (13) and (14), let us use the simplification of optical phonons with a peak frequency ω_0 and small dispersion $\sigma \ll \omega_0$, with an average coupling constant g. If the density of states considered is that of a Gaussian peaked at ω_0 and width σ, Eqs. (13) and (14) (in the continuum limit) have the forms

$$\begin{aligned}\mathscr{B}(t) = {} & g^2\hbar^2\omega_0^2 e^{-\frac{\sigma^2 t^2}{2}} \\ & \times \left\{ \coth\left(\frac{\beta\hbar\omega_0}{2}\right) \left[\left(1 + \frac{\sigma^2}{\omega_0^2} - \frac{\sigma^4 t^2}{\omega_0^2}\right) \cos(\omega_0 t) - 2\frac{\sigma^2}{\omega_0} t \sin(\omega_0 t) \right] \right. \\ & \left. + i \left[\left(1 + \frac{\sigma^2}{\omega_0^2} - \frac{\sigma^4 t^2}{\omega_0^2}\right) \sin(\omega_0 t) + 2\frac{\sigma^2}{\omega_0} t \cos(\omega_0 t) \right] \right\},\end{aligned} \tag{15}$$

in the weak-coupling case [30] and

$$\mathscr{B}(t) = u^2 e^{-g^2 \coth\left(\frac{\beta\hbar\omega_0}{2}\right)\left(1 - e^{-\frac{\sigma^2 t^2}{2}} \cos\omega_0 t\right)} e^{ig^2 e^{-\frac{\sigma^2 t^2}{2}} \sin\omega_0 t}, \tag{16}$$

in the strong-coupling case [31], respectively.

It is expected that the memory functions resulting from the use of Eqs. (15) and (16) would decay to zero at long times due to the interaction of the system with the thermal reservoir. However, the linear interactions considered in this study cannot broaden the zero-phonon lines present in optical spectra [28,32], and the memories produced never quite decay to zero, oscillating about a nonzero value determined by the microscopically specified parameters. The solution to this problem, discussed in the literature earlier [28,29], lies in the unavoidable introduction of sources of disorder not taken explicitly into account in the microscopic description of the Hamiltonian [20–22,28]. This is done through the incorporation of an extra decay factor introduced into the memories [29]. In all three systems, the bath correlation functions Eqs. (13) and (14) may be thus considered as being calculated for a single mode of vibrational mode and multiplied by a time-dependent factor $f(t)$ which takes into account both the phonon spectral line shape and sources of disorder mentioned above. This allows for Eqs. (15) and (16) to be represented as

$$\mathscr{B}(t) = g^2\hbar^2\omega_0^2 \left[\coth\left(\frac{\beta\hbar\omega_0}{2}\right) \cos(\omega_0 t) + i \sin(\omega_0 t) \right] f(t), \tag{17}$$

and

$$\mathscr{B}(t) = u^2 e^{-g^2 \coth\left(\frac{\beta\hbar\omega_0}{2}\right)(1 - \cos\omega_0 t)} e^{ig^2 \sin\omega_0 t} f(t), \tag{18}$$

respectively.

2.3. Nonmonotonic temperature dependence of the rates

The most convenient representation of $f(t)$ is the exponential $e^{-\alpha t}$ which is compatible with the derivation of the GME in the presence of disorder [33,34]. It represents quite well the time behavior of all three system observables as our numerical computations have shown, and the corresponding memories in each coupling regime, have the forms

$$\Gamma\phi_\pm(t) = 2g^2\omega_0^2 \left[\coth\left(\frac{\beta\hbar\omega_0}{2}\right) \cos(\omega_0 t) \cos(\Omega t) \mp \sin(\omega_0 t) \sin(\Omega t) \right] e^{-\alpha t} \tag{19a}$$

for the weak (single-phonon) interaction, and

$$\Gamma\phi_\pm(t) = 2\frac{u^2}{\hbar^2} e^{-g^2 \coth\left(\frac{\beta\hbar\omega_0}{2}\right)(1 - \cos\omega_0 t)} \cos\left[g^2 \sin(\omega_0 t) \pm \Omega t\right] e^{-\alpha t}, \tag{19b}$$

for the strong (multiphonon) interaction. Here Ω and Γ may be replaced, respectively, by the characteristic frequency and relaxation rate of whichever system we are analyzing. The Γ's are found by taking the Fourier transform of the specified

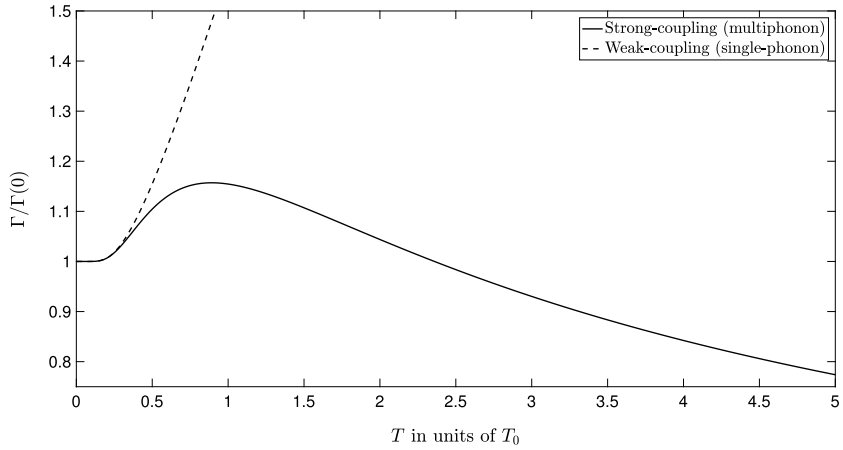

Fig. 1. Temperature dependence of the relaxation rates Γ for both weak and strong interactions. T is plotted in units of $T_0 = \hbar\omega_0/k_B$. The system, as described in the text, is a harmonic oscillator of characteristic frequency Ω in strong ($g = 2$) and weak ($g = 0.02$) interaction with optical phonons of peak frequency $\omega_0 = \Omega + \alpha/2$ and narrow dispersion $\alpha/\Omega = 0.01$. A monotonic increase of the rate with increasing T is observed for the weak-coupling (single-phonon) case. In the strong-coupling (multiphonon) case, the rate exhibits distinctive nonmonotonic behavior with increasing T, making the T interval over which the rate is observed of particular importance.

memories in Eqs. (19) and are

$$\Gamma = 2\frac{u^2}{\hbar^2}e^{-g^2\coth\left(\frac{\beta\hbar\omega_0}{2}\right)}\sum_{\ell=-\infty}^{\infty} I_\ell\left[2g^2 n\left(\omega_0\right)\right]\sum_{k=0}^{\infty}\frac{g^{2k}}{k!}\frac{\alpha}{\alpha^2+\left[(k+\ell)\omega_0-\Omega\right]^2} \tag{20}$$

in the multiphonon (strong-coupling) interaction case, and

$$\Gamma = 2g^2\omega_0^2\left\{\left[n\left(\omega_0\right)+1\right]\frac{\alpha}{\alpha^2+\left(\omega_0-\Omega\right)^2}+n\left(\omega_0\right)\frac{\alpha}{\alpha^2+\left(\omega_0+\Omega\right)^2}\right\} \tag{21}$$

in the single-phonon (weak-coupling) interaction case, respectively. While the case of weak interaction with the bath (single-phonon interaction) results in an Arrhenius behavior wherein the rate is activated and increases with increasing T, in the case of a strong-coupling (multiphonon) interaction, a nonmonotonic behavior of the rate is observed. Thus, whether the relaxation rate increases or decreases with T is determined by what T-interval is used for the measurement (see Fig. 1).

The rest of the investigation in this paper consists of (i) the substitution of the two bath correlation functions, one for the single-phonon interaction case, Eq. (15), and the other for the multiphonon case, Eq. (16), into the $\mathscr{W}(t)$ function prescriptions in Eqs. (11) to obtain the corresponding upward and downward memories $\phi_\pm(t)$ for each system, (ii) the use of these common ϕ's and the separate $|\langle M|V_S|N\rangle|^2$ for each system in the probability equations Eqs. (1)–(3) and their observable consequences, $p(t)$ for the dimer, $v(t)$ for the charged particle, and $E(t)$ for the harmonic oscillator, and (iii) examination of the behavior of the three observables for the three systems with respect to the variation of microscopic parameters.

3. Application of the Theory I: the simple nonresonant dimer

As perhaps the simplest possible case for our study of the approach to equilibrium, we investigate in this section the nonresonant dimer with energy difference 2Δ. Its spectrum is not infinite as that of the charged particle ($M = -\infty, \ldots, \infty$) or semi-infinite as that of the vibrating molecule ($M = 0, \ldots, \infty$), but consists of only two states ($M = 1, 2$). One of the reasons for this study is that the dimer serves as a tutorial system which exhibits the principal features of the other two systems. Another reason has to do with the equienergetic spectrum of the harmonic oscillator that may produce undesirable harmonics in predicted signals. The energy difference between the two states of the anharmonic oscillator that are involved in the process being probed is often large. In such cases the contribution to relaxation from states other than two to turn out to be negligible. It is then preferable, even perhaps advisable [35], to model relaxation experiments via anharmonic oscillators and therefore via the nonresonant dimer.

An earlier treatment [6] of the nonresonant dimer results in Eq. (1) whose solution may be written as

$$p(t) = p(0)\mu(t) + \int_0^t ds\, \Xi\,(t-s)\left[\mu\,(s)-1\right], \tag{22}$$

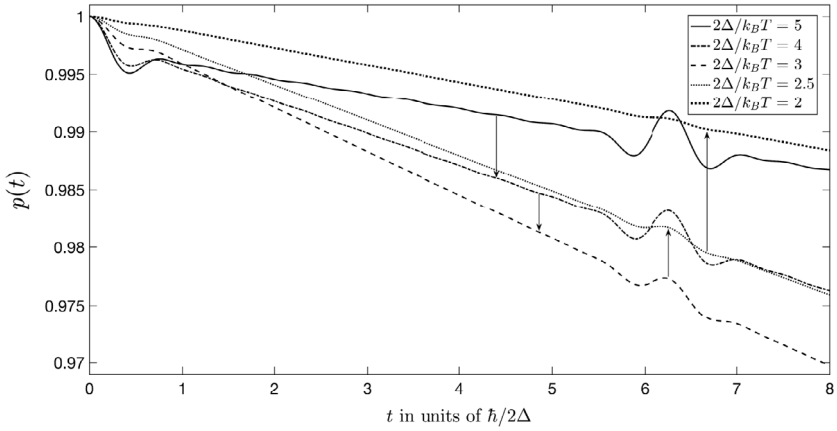

Fig. 2. Time evolution of the occupation probability difference plotted as a function of time t in units of $\hbar/2\Delta$ for the nondegenerate dimer in strong interaction ($g = 2$) with optical phonons of peak frequency $\omega_0 = 2\Delta/\hbar$ and narrow dispersion $\hbar\alpha/2\Delta = 0.01$ for various T: values for $2\Delta/k_BT$ are shown in the legend. Initial revival oscillations damp out as T is increased, decaying to silent runs. Striking is the nonmonotonic effect: as T increases, the time evolution curve moves down and then moves up (as the arrows show) as T is increased further. One also observes a decrease in the amplitude of the periodic revivals as T increases.

for the difference in the occupation probability $p(t) = P_1(t) - P_2(t)$, where $\Xi(t)$ and $\mu(t)$ are the Laplace inverses of

$$\tilde{\Xi}(\epsilon) = \frac{\widetilde{\phi}_D(\epsilon)}{\widetilde{\phi}_S(\epsilon)} \qquad \text{and} \qquad \tilde{\mu}(\epsilon) = \frac{1}{\epsilon + F_{21}\widetilde{\phi}_S(\epsilon)}, \tag{23}$$

respectively. At long times, $p(t)$ approaches $-\tanh(\Delta/k_BT)$ as expected from detailed balance. Here ϕ_S and ϕ_D are the sum and difference[2] of the microscopic memories ϕ, respectively, *i.e.*, $\phi_\nu = \phi_- \pm \phi_+$, where the '+' (sum) corresponds to $\nu = S$ and the '−' (difference) to $\nu = D$.

On applying the microscopic memories we have calculated in the present paper in Section 2, the sum and difference of the memories in the multiphonon (strong-coupling) case turn out to have the form

$$F_{21}\phi_\nu(t) = 4\frac{u^2}{\hbar^2} e^{-g^2 \coth(\beta\hbar\omega_0/2)(1-\cos\omega_0 t)} \Lambda\left(g^2 \sin\omega_0 t\right) \Lambda\left(2\Delta t/\hbar\right) e^{-\alpha t}, \tag{24}$$

where if $\nu = S$ (sum), the function $\Lambda(x)$ is $\cos(x)$ and if $\nu = D$ (difference) is $\sin(x)$. The corresponding Laplace transform of Eq. (24) is

$$F_{21}\tilde{\phi}_\nu(\epsilon) = 4\frac{u^2}{\hbar^2} e^{-g^2 \coth(\beta\hbar\omega_0/2)} \times \sum_{\ell=-\infty}^{\infty} \frac{I_\ell\left[g^2 \operatorname{csch}\left(\frac{\beta\hbar\omega_0}{2}\right)\right] e^{\ell\frac{\beta\hbar\omega_0}{2}} (\epsilon+\alpha)\, \chi_\ell(\epsilon)}{\left[(\epsilon+\alpha)^2 + (\ell\omega_0 + 2\Delta/\hbar)^2\right]\left[(\epsilon+\alpha)^2 + (\ell\omega_0 - 2\Delta/\hbar)^2\right]}, \tag{25}$$

where if $\nu = S$, the function $\chi_\ell(\epsilon)$ is $(2\Delta/\hbar)^2 + \ell^2\omega_0^2 + (\epsilon+\alpha)^2$ and if $\nu = D$ it is $2\ell\omega_0(2\Delta/\hbar)$. The passage from Eqs. (24) to (25) uses an expansion of the exponential of the trigonometric function into an infinite series of modified Bessel functions.

Interesting features appear in the time evolution of $p(t)$ in the multiphonon (strong-coupling) interaction case. In Fig. 2, $p(t)$ is plotted with respect to time in units of $\hbar/2\Delta$ for the case of strong coupling with a bath of optical phonons of peak frequency $\omega_0 = 2\Delta/\hbar$. We notice both the nonmonotonicity effect brought about by the associated relaxation rate F_{21} calculated in Eq. (20) with $\hbar\Omega = 2\Delta$ and revivals known to exist in spin-boson systems [36] at short times. At lower temperatures oscillations, silent runs, and revivals are evident, as discussed in spin-boson investigations [36]. As T is increased, the revivals prevalent at vanishing T begin to dissipate with increasing T. The nonmonotonicity effect present is depicted as the arrows show in Fig. 2: $p(t)$ decreases as T increases from 1/5 to 1/3 in units of $2\Delta/k_B$, and begins to increase as T increases further from 1/3 to 1/2 in those units.

In the case of the single-phonon (weak-coupling) interaction, the bath contribution to the interaction includes a shift created by the intersite matrix element u such that the bath contribution to the interaction in Eq. (5b) is written as

$$V_B = u + \sum_q g_q\hbar\omega_q\left(b_q + b_q^\dagger\right). \tag{26}$$

[2] The notation $\phi_D(t)$ instead of $\phi_\Delta(t)$ is used for the memory difference unlike in Eq. (9) of Ref. [10].

Here u is also treated perturbatively to yield a bath correlation function of the form

$$\mathscr{B}(t) = u^2 + (g^2/2)\hbar^2\omega_0^2 n(\omega_0)\left(e^{\beta\hbar\omega_0}e^{i\omega_0 t} + e^{-i\omega_0 t}\right) \tag{27}$$

and memories with an incorporated disorder term ($e^{-\alpha t}$) of the form

$$F_{21}\phi_{\pm}(t) = 2\frac{u^2}{\hbar^2}\cos(2\Delta t/\hbar)\, e^{-\alpha t} + g^2\omega_0^2 n(\omega_0)\left[e^{\beta\hbar\omega_0}\cos(2\Delta t/\hbar \pm \omega_0 t) + \cos(2\Delta t/\hbar \mp \omega_0 t)\right] e^{-\alpha t}. \tag{28}$$

The sum and difference of the memories in Eqs. (28) and their Laplace transforms have the forms

$$F_{21}\phi_{\nu}(t) = 4\frac{u^2}{\hbar^2}\delta_{\nu,S}\cos(2\Delta t/\hbar)\, e^{-\alpha t} + 2g^2\omega_0^2\,\Upsilon(\omega_0)\Lambda(\omega_0 t)\,\Lambda(2\Delta t/\hbar)\, e^{-\alpha t}, \tag{29}$$

and

$$F_{21}\tilde{\phi}_{\nu}(\epsilon) = 4u^2\delta_{\nu,S}\frac{\epsilon+\alpha}{\hbar^2(\epsilon+\alpha)^2 + 4\Delta^2} + \frac{2g^2\omega_0^2\,\Upsilon(\omega_0)(\epsilon+\alpha)\chi_1(\epsilon)}{\left[(\epsilon+\alpha)^2 + (\omega_0 + 2\Delta/\hbar)^2\right]\left[(\epsilon+\alpha)^2 + (\omega_0 - 2\Delta/\hbar)^2\right]}, \tag{30}$$

respectively, where the functions $\Upsilon(x)$ and $\delta_{\nu,S}$ are $\coth(\beta\hbar x/2)$ and 1 if $\nu = S$ (sum), respectively, and 1 and 0 if $\nu = D$ (difference) and $\Lambda(x)$ and $\chi_\ell(x)$ are as for Eqs. (24) and (25), respectively. We calculate the behavior of the occupation probability in one of the two extreme time limits by following the Tiwari–Kenkre analysis [6]. In the short-time limit, $\omega_0 t \ll 1$, the difference in the memories approaches 0 while the sum may be approximated to

$$F_{21}\phi_S(t) \approx 4\left(u^2/\hbar^2\right)\cos(2\Delta t/\hbar) + 2g^2\omega_0^2\coth(\beta\hbar\omega_0/2)\cos(2\Delta t/\hbar)\,. \tag{31}$$

The resulting short-time behavior of the occupation probability difference is both a temperature- and interaction-dependent oscillation

$$p(t\to 0) = \langle p\rangle + (1-\langle p\rangle)\cos\left(2\Delta t/\hbar\sqrt{\langle p\rangle}\right), \tag{32}$$

around the average value $\langle p\rangle$ given by

$$\langle p\rangle = \frac{\Delta^2}{\Delta^2 + u^2 + \frac{(g\hbar\omega_0)^2}{2}\coth(\beta\hbar\omega_0/2)} \tag{33}$$

If there is no interaction with the bath, *i.e.*, $g = 0$, $\langle p\rangle$ reduces to the value given earlier in Ref. [6] obtained for an isolated nondegenerate dimer. As T increases, the shifted equilibrium position approaches zero, while the frequency of oscillation between the two states in the occupation probability difference at short times becomes infinite.

4. Application of the Theory II: charge in a strong electric field

Let us now consider the dynamics of a particle of charge q, moving in a 1-dimensional crystal of lattice constant a in the direction of a strong applied electric field E, as a result of the interaction with a thermal reservoir. In a recent analysis [10], Eq. (2) was used to calculate the time-evolution of the average velocity of the charged particle,

$$v(t) = \frac{d\langle M(t)\rangle}{dt} = \int_0^t ds\,\varkappa\phi_D(s) \tag{34}$$

suppressing, for simplicity, the multiplicative factor of the lattice constant a. The ϕ's used were phenomenological. We now apply the present theory to this system by obtaining the velocity from the microscopic memories obtained here in Eqs. (19). For this example, $\Omega = \mathcal{E}/\hbar$ and $\Gamma = \varkappa$. The memory difference ϕ_D is given by

$$\varkappa\phi_D(t) = 8\frac{u^2}{\hbar^2}e^{-g^2\coth\left(\frac{\beta\hbar\omega_0}{2}\right)}\sum_{\ell=1}^{\infty} I_\ell\left[g^2\,\mathrm{csch}\left(\frac{\beta\hbar\omega_0}{2}\right)\right]\sinh\left(\ell\frac{\beta\hbar\omega_0}{2}\right) \times \sin(\ell\omega_0 t)\sin(\mathcal{E}t/\hbar)\, e^{-\alpha t} \tag{35a}$$

in the multiphonon case, and

$$\varkappa\phi_D(t) = 4g^2\omega_0^2\sin(\omega_0 t)\sin(\mathcal{E}t/\hbar)\, e^{-\alpha t} \tag{35b}$$

in the single-phonon case, respectively.

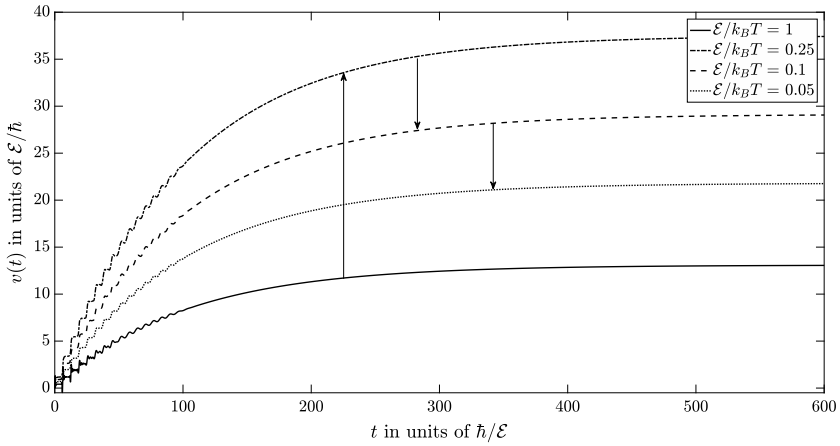

Fig. 3. Staircase behavior and the nonmonotonicity effect seen in the time dependence of the velocity of a charged particle of characteristic energy $\mathcal{E}$ moving along the sites of a crystal, while in strong interaction ($g = 2$) with optical phonons of peak frequency $\omega_0 = \mathcal{E}/\hbar$ and narrow dispersion $\alpha = 0.01\,\mathcal{E}/\hbar$. As $\mathcal{E}/k_BT$ increases (T is decreased), the velocity rises and then falls. As time increases, the steady-state (incoherent limit) value of the velocity is reached. Periodic *kinks* are observed about the step-like progression of the velocity at shorter times for lower T. The kinks dissipate with increasing time and increasing temperature.

The result for the velocity in the multiphonon (strong-coupling) interaction case is

$$\begin{aligned} v(t) = 2\frac{u^2}{\hbar^2} e^{-g^2 \coth\left(\frac{\beta\hbar\omega_0}{2}\right)} \\ \times \sum_{\ell=1}^{\infty} I_\ell \left[g^2 \operatorname{csch}\left(\frac{\beta\hbar\omega_0}{2}\right)\right] \sinh\left(\ell\frac{\beta\hbar\omega_0}{2}\right) \\ \times \left[f_{\ell,-}(\omega_0, t) - f_{\ell,-}(\omega_0, 0) - f_{\ell,+}(\omega_0, t) + f_{\ell,+}(\omega_0, 0)\right], \end{aligned} \tag{36}$$

where

$$f_{\ell,\pm}(\omega_0, t) = e^{-\alpha t} \frac{(\ell\omega_0 \pm \mathcal{E}/\hbar)\sin(\ell\omega_0 t \pm \mathcal{E}/\hbar t) - \alpha\cos(\ell\omega_0 t \pm \mathcal{E}/\hbar t)}{\alpha^2 + (\ell\omega_0 \pm \mathcal{E}/\hbar)^2}, \tag{37}$$

while in the single-phonon (weak-coupling) interaction case, the velocity has the temperature-independent form

$$v(t) = 4g^2\omega_0^2 \left[f_{1,-}(\omega_0, t) - f_{1,-}(\omega_0, 0) - f_{1,+}(\omega_0, t) + f_{1,+}(\omega_0, 0)\right]. \tag{38}$$

Initially the velocity is zero in both regimes, but as time progresses, the time-dependent components (the $f_{\ell,\pm}(\omega_0, t)$ terms) produce a step-wise rise in the velocity, the frequency of which is determined by the sum and difference of the system and bath frequencies, $\mathcal{E}/\hbar$ and ω_0, respectively. The step-like nature of the time-evolution of the velocity is reminiscent of, and related to, similar effects seen in the theory of dynamic localization [37–39]. In both regimes, the steps dissipate as the velocity approaches the steady-state value which is expected [10] to approach $\varkappa\left(1 - e^{-\beta\mathcal{E}}\right)$, where $\varkappa$ is the T-dependent relaxation rate associated with each interaction.

In the strong-coupling regime, a temperature dependence for all time exists in the hyperbolic cotangent in the first exponent as well as in the terms inside the sum. When combined, the terms produce a nonmonotonic T dependence in the behavior of the velocity, the degree of the nonmonotonicity being determined by the relative magnitude of the corresponding time-dependent terms in Eq. (38). In Fig. 3, this nonmonotonic effect can be seen in the approach to steady state of the velocity with time. In the multiphonon (strong-coupling) case, the velocity approaches

$$\begin{aligned} v(t \to \infty) = \frac{2u^2}{\hbar^2} e^{-g^2 \coth\left(\frac{\beta\hbar\omega_0}{2}\right)} \sum_{\ell=-\infty}^{\infty} I_\ell \left[2g^2 n(\omega_0)\right] \\ \times \sum_{k=0}^{\infty} \frac{g^{2k}}{k!} \left[\frac{\alpha}{\alpha^2 + \left[(k+\ell)\omega_0 - \mathcal{E}/\hbar\right]^2} - \frac{\alpha}{\alpha^2 + \left[(k+\ell)\omega_0 + \mathcal{E}/\hbar\right]^2}\right] \end{aligned} \tag{39}$$

wherein the expression can be shown to have a direct dependence on the associated relaxation rate (Eq. (20) with $\Omega = \mathcal{E}/\hbar$) and approaches the expected steady-state value.

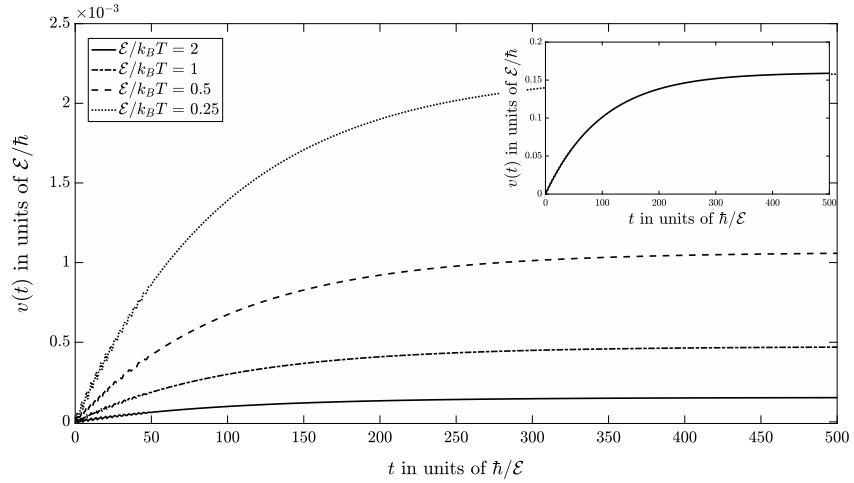

Fig. 4. Results for two-phonon interaction with the bath. Plotted is the time dependence of the velocity for different values $\mathcal{E}/k_BT$ as shown. This is the weak interaction case, $g = 0.02$. The inset shows the temperature-independent velocity that arises from interaction with a single phonon band of peak frequency $\omega_0 = \mathcal{E}/\hbar$. In the main figure the two phonon bands have central frequencies ω_1 and ω_2, all three phonon bands having a narrow dispersion $\alpha = 0.01\,\mathcal{E}/\hbar$. Unlike in the inset, the long-time saturation value of the velocity in the main figure increases with increasing T.

The steady-state value of the velocity in the *single-phonon* (weak-coupling) case, on the other hand, has a temperature independent form

$$v(t \to \infty) = 4g^2\omega_0^2 \left[\frac{\alpha}{\alpha^2 + (\omega_0 - \mathcal{E}/\hbar)^2} - \frac{\alpha}{\alpha^2 + (\omega_0 + \mathcal{E}/\hbar)^2} \right]. \tag{40}$$

When written in terms of its associated relaxation rate (Eq. (21) with $\Omega = \mathcal{E}/\hbar$), this can be easily shown to reproduce the expected steady-state value of $\varkappa \left(1 - e^{-\beta\mathcal{E}}\right)$. One of the factors responsible for the temperature independence evident in Eq. (40) is that there is only a single phonon band involved. We therefore investigated the case that two phonon bands are involved, following the description detailed in Ref. [27]. The result is displayed in Fig. 4. The inset shows the T independence arising from the single phonon band. The main figure, however, displays the expected dependence on T. The two phonon bands are peaked at frequency ω_1 and ω_2, respectively, and are of narrow width. The resulting memories are of the form

$$\begin{aligned} \varkappa\phi_{\pm}(t) = {} & 2g_1^2 g_2^2 \hbar^2 \omega_1^2 \omega_2^2 n(\omega_1) n(\omega_2) e^{-\alpha t} \\ & \times \Big\{ e^{\beta\hbar(\omega_1+\omega_2)} \cos\left[(\omega_1 + \omega_2 \pm \mathcal{E}/\hbar)\, t\right] + \cos\left[(\omega_1 + \omega_2 \mp \mathcal{E}/\hbar)\, t\right] \\ & \quad + e^{\beta\hbar\omega_1} \cos\left[(\omega_1 - \omega_2 \pm \mathcal{E}/\hbar)\, t\right] + e^{\beta\hbar\omega_2} \cos\left[(\omega_1 - \omega_2 \mp \mathcal{E}/\hbar)\, t\right] \Big\}, \end{aligned} \tag{41}$$

with the difference having an T dependence involving the two frequencies,

$$\varkappa\phi_D(t) = 4g_1^2 g_2^2 \hbar^2 \omega_1^2 \omega_2^2 \sin\left(\mathcal{E}t/\hbar\right) e^{-\alpha t} \sum_{i \neq j}^{2} \coth\left(\frac{\beta\hbar\omega_i}{2}\right) \cos\left(\omega_i t\right) \sin\left(\omega_j t\right). \tag{42}$$

It is easily seen that this T dependence is carried out into the expression for the velocity

$$\begin{aligned} v(t) = {} & g_1^2 g_2^2 \hbar^2 \omega_1^2 \omega_2^2 \sum_{k=0}^{1} \left[\coth\left(\frac{\beta\hbar\omega_2}{2}\right) + (-1)^k \coth\left(\frac{\beta\hbar\omega_1}{2}\right) \right] \\ & \times \Big\{ f_{1,-}(x_k, t) - f_{1,-}(x_k, 0) - f_{1,+}(x_k, t) + f_{1,+}(x_k, 0) \Big\}, \end{aligned} \tag{43}$$

where $f_{\ell,\pm}(x_k, t)$ is as in Eq. (37) with $x_k = \omega_1 + (-1)^k\omega_2$. The temperature dependence present in the expression for the velocity in this *weak* interaction with two phonons displays a monotonic behavior with T (see Fig. 4).

5. Application of the Theory III: vibrationally relaxing molecule

As our third example of the application of our theory, we consider a molecule, modeled as a harmonic oscillator of frequency Ω, undergoing vibrational relaxation because of its interaction with a bath in which it is embedded. Traditionally,

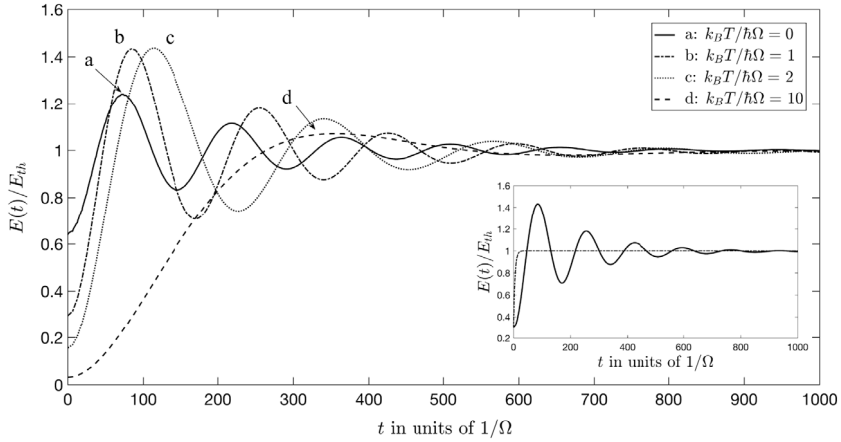

Fig. 5. Nonmonotonic temperature (T) dependence of the energy of the relaxing molecule of characteristic frequency Ω in strong interaction ($g = 2$) with optical phonons of peak frequency $\omega_0 = \Omega + \alpha/2$ and narrow dispersion $\alpha/\Omega = 0.01$. Plots are shown of $E(t)$ scaled to its thermal equilibrium value of E_{th} for varying T, *i.e.*, for various values of $\beta\hbar\Omega$, (a), (b), (c), (d), as shown in the legend. A striking dependence is observed as T is increased. The values of T in units of T_0 for curve (a) is 0, for curve (b) is 1, for curve (c) is 2, and for curve (d) is 10, with the corresponding peaks being shown by arrows. The peak values increase from (a) to (b) to (c) but decrease from (c) to (d). The lower right inset shows the difference between the incoherent limit (Bethe-Teller) (dashed line) and our GME predictions (solid line) for one representative case, $\hbar\Omega/k_BT = 1$.

such relaxation has been studied via the Montroll–Shuler equation (MSE) [11]. We use the generalization of that equation given recently by Kenkre and Chase [10]. The latter authors have shown that one can derive from Eq. (3) the result that the molecular energy $E(t) = \hbar\Omega\sum_M (M + 1/2)\, P_M(t)$ obeys

$$E(t) = E(0)\eta(t) + E_{th}\int_0^t ds\, \xi(t-s)\,[1-\eta(s)] \tag{44}$$

where $E(0)$ is the initial energy of the system, $E_{th} = \frac{\hbar\Omega}{2}\coth\left(\frac{\beta\hbar\Omega}{2}\right)$ is its thermal or steady-state value, and $\eta(t)$ and $\xi(t)$ are the Laplace inverses of

$$\tilde{\eta}(\epsilon) = \frac{1}{\epsilon + \kappa\tilde{\phi}_D(\epsilon)} \qquad \text{and} \qquad \tilde{\xi}(\epsilon) = \frac{\tilde{\phi}_S(\epsilon)}{\tilde{\phi}_D(\epsilon)}\tanh\left(\frac{\beta\hbar\Omega}{2}\right), \tag{45}$$

respectively. Eq. (44) extends to situations of arbitrary coherence the traditional (incoherent) result

$$E(t) = E(0)e^{-\kappa\left(1-e^{-\beta\hbar\Omega}\right)t} + E_{th}\left[1 - e^{-\kappa\left(1-e^{-\beta\hbar\Omega}\right)t}\right]. \tag{46}$$

That result is recovered from Eq. (44) in the Markoffian limit that $\tilde{\phi}(\epsilon)$'s are replaced by the corresponding $\tilde{\phi}(0)$'s.

We now use in Eqs. (44), (45) the microscopic memories we have derived in Eqs. (19) to investigate whether any interesting effects of T and other parameters emerge. In the multiphonon (strong-coupling) case, the $\phi_S(t)$ and $\phi_D(t)$ are

$$\kappa\phi_\nu(t) = 4\frac{u^2}{\hbar^2}e^{-g^2\coth(\beta\hbar\omega_0/2)(1-\cos\omega_0 t)}\,\Lambda\left(g^2\sin\omega_0 t\right)\Lambda\left(\Omega t\right)e^{-\alpha t}, \tag{47}$$

where if $\nu = S$ (sum), the function $\Lambda(x)$ is $\cos(x)$ and if $\nu = D$ (difference) is $\sin(x)$ and in the single-phonon (weak-coupling) case the $\phi_S(t)$ and $\phi_D(t)$ are

$$\kappa\phi_\nu(t) = 4g^2\omega_0^2\,\Upsilon(\omega_0)\Lambda\left(\omega_0 t\right)\Lambda\left(\Omega t\right)e^{-\alpha t}, \tag{48}$$

where the function $\Upsilon(x)$ is $\coth\left(\beta\hbar x/2\right)$ if $\nu = S$ (sum) and 1 if $\nu = D$ (difference).

While a temperature dependence exists in both the sum and difference of the memories in the multiphonon interaction case, it is clear from the expressions in Eqs. (48) that the difference of the memories, and hence $\eta(t)$, is T-independent in the single-phonon case. This inherent T-dependence disparity in the initial behavior of $E(t)$ signals a difference in the overall effect of T on the relaxation behavior of the oscillator in the two regimes. This is expected from the T-dependent behavior of the corresponding relaxation rates, nonmonotonic in the strong-coupling (multiphonon) case, Eq. (20), and Arrhenius in the weak-coupling (single-phonon) case, Eq. (21).

The nonmonotonic effect with T in the multiphonon interaction case becomes more discernible in Fig. 5 which shows the time evolution of the average energy resulting from the substitution of the memories in Eq. (24) into Eq. (44) for various

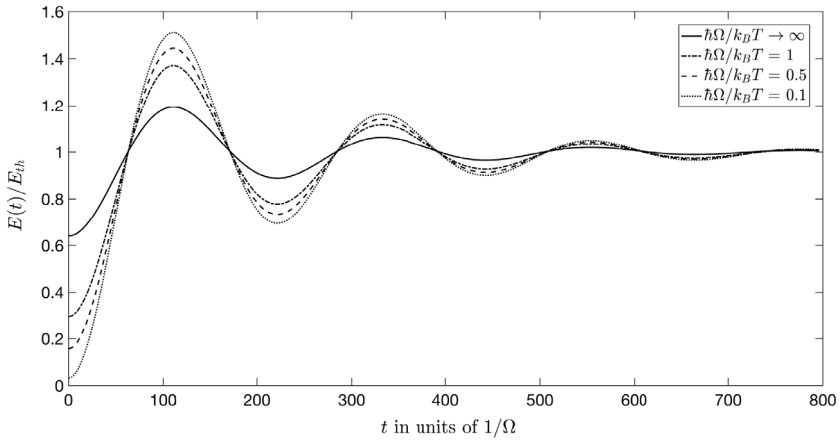

Fig. 6. Absence of interesting results such as nonmonotonicity for weak-coupling (single-phonon interactions). The time evolution of the average energy of a harmonic oscillator of characteristic frequency Ω in weak interaction ($g = 0.02$) with optical phonons of peak frequency $\omega_0 = \Omega + \alpha/2$ and narrow dispersion $\alpha/\Omega = 0.01$ is plotted with respect to time t, for varying T. As T is increased, the average energy initially rises above the incoherent limit value, with oscillations decaying faster to E_{th}. The frequency of oscillation remains the same for all T, while the amplitude shows a direct T dependence, increasing with increasing T.

values of T. The inset shows a comparison of the coherent (oscillatory) behavior of the energy predicted by the GME of Eq. (3) to the incoherent (non-oscillatory) behavior predicted by the MSE [11] for one temperature. For each value of T shown in the main part of Fig. 5, the approach to equilibrium of the energy is dominated by initial T-dependent oscillations about the steady-state value E_{th}, and then dissipating to it. The nonmonotonic T dependence is seen clearly in the rise and fall of the peak amplitude of the energy as T is increased. As the figure shows, the peak value of the energy rises initially (from a to b) with increasing T and then falls (from c to d) as the period of oscillation increases monotonically. This nonmonotonic behavior may be explained by the temperature dependence of the relaxation rate in Eq. (20).

Another noteworthy feature seen, particularly at low T, is the existence of periodic *kinks* observed along the main curve of $E(t)$, the kink amplitudes dissipating with the progression of time (see Fig. 8). As T is increased, the time interval over which the kinks are visible is decreased. These kinks are related to the revivals which are known to exist in spin-boson systems [36,40].

In the Laplace domain, Eqs. (47) and (48) have the forms, respectively,

$$\kappa\tilde{\phi}_\nu(\epsilon) = 4\frac{u^2}{\hbar^2}e^{-g^2\coth(\beta\hbar\omega_0/2)} \sum_{\ell=-\infty}^{\infty} \frac{I_\ell\left[g^2\mathrm{csch}\left(\frac{\beta\hbar\omega_0}{2}\right)\right]e^{\ell\frac{\beta\hbar\omega_0}{2}}(\epsilon+\alpha)\,\chi_\ell(\epsilon)}{\left[(\epsilon+\alpha)^2+(\ell\omega_0+\Omega)^2\right]\left[(\epsilon+\alpha)^2+(\ell\omega_0-\Omega)^2\right]} \tag{49}$$

and

$$\kappa\tilde{\phi}_\nu(\epsilon) = 4g^2\omega_0^2\,\Upsilon(\omega_0)\frac{(\epsilon+\alpha)\chi_1(\epsilon)}{\left[(\epsilon+\alpha)^2+(\omega_0+\Omega)^2\right]\left[(\epsilon+\alpha)^2+(\omega_0-\Omega)^2\right]}. \tag{50}$$

Here, if $\nu = S$, the function $\chi_\ell(\epsilon)$ is $\Omega^2+\ell^2\omega_0^2+(\epsilon+\alpha)^2$ and if $\nu = D$ it is $2\ell\omega_0\Omega$. It can be shown, either numerically in the multiphonon case or analytically in the single-phonon case, that, in the limit $\epsilon \to 0$, the ratio of the Laplace transform of the sum and difference of these microscopically derived memories approaches $\coth(\beta\hbar\Omega/2)$.

In the case of weak interaction also, one notices initial oscillations about, and dissipating to, the steady-state value E_{th} at long times with temperature-dependent amplitudes (see Fig. 6), the energy in this case having the analytic form

$$E(t) = \left[E(0) - E_{th}\frac{\tanh\left(\frac{\beta\hbar\Omega}{2}\right)}{\tanh\left(\frac{\beta\hbar\omega_0}{2}\right)}\frac{\Omega^2+\omega_0^2+\alpha^2}{2\omega_0\Omega}\right]\eta(t) + E_{th}\frac{\tanh\left(\frac{\beta\hbar\Omega}{2}\right)}{\tanh\left(\frac{\beta\hbar\omega_0}{2}\right)}\frac{\Omega^2+\omega_0^2+\alpha^2}{2\omega_0\Omega}, \tag{51}$$

where

$$\eta(t) = e^{-\alpha t}\mathcal{L}^{-1}\left\{\frac{\left[\epsilon^2 + (\omega_0+\Omega)^2\right]\left[\epsilon^2 + (\omega_0-\Omega)^2\right]}{\left[\epsilon^2 + (\omega_0+\Omega)^2\right]\left[\epsilon^2 + (\omega_0-\Omega)^2\right](\epsilon-\alpha) + 8g^2\omega_0^3\Omega\epsilon}\right\}. \tag{52}$$

While no general analytic solution exists for $\eta(t)$, it is evident that no T dependence exists in $\eta(t)$ for the single-phonon interaction case, and that the behavior of $\eta(t)$ is of decaying oscillatory form as expected.

5.1. Introduction of a relaxation memory and an effective rate

As seen in the previous sections, the relaxation rate can be obtained through the Fourier transform of the microscopically derived bath correlation function $\mathscr{B}(t)$ evaluated at the oscillator frequency. In this section, we develop an approach in terms of a relaxation memory and an effective rate. The incoherent result [11], Eq. (46), may be rewritten as

$$\frac{E(t) - E_{th}}{E(0) - E_{th}} = e^{-\kappa\left(1-e^{-\beta\hbar\Omega}\right)t} \tag{53}$$

to emphasize that the effective rate of relaxation is $\kappa\left(1 - e^{-\beta\hbar\Omega}\right)$. Although the generalization in Ref. [10] reflected in Eq. (44) results in a non-exponential time-dependence of the left hand side of Eq. (53), its Laplace transform can always be expressed as

$$\frac{\tilde{E}(\epsilon) - E_{th}/\epsilon}{E(0) - E_{th}} = \frac{1}{\epsilon + \tilde{\zeta}(\epsilon)}, \tag{54}$$

through the introduction of the Laplace transform of a *relaxation memory* $\zeta(t)$. In the incoherent Master equation approximation, $\zeta(t)$ is $\kappa\left(1 - e^{-\beta\hbar\Omega}\right)\delta(t)$, while in the general case, $\zeta(t)$ describes coherent oscillations present in the exact result of $E(t)$ obtained from Eq. (44). The memory is found through the corresponding relation of the energy in Eq. (44) in the Laplace domain as

$$\tilde{\zeta}(\epsilon) = \frac{\epsilon\left[E(0) - E_{th}\tilde{\xi}(\epsilon)\right]\left[1 - \epsilon\tilde{\eta}(\epsilon)\right]}{E(0) - E_{th} - \left[E(0) - E_{th}\tilde{\xi}(\epsilon)\right]\left[1 - \epsilon\tilde{\eta}(\epsilon)\right]}. \tag{55}$$

We now provide a formula for an *effective* rate of relaxation in the presence of non-exponential time evolution of the energy $E(t)$ that can take into account the consequences of all non-exponential features including oscillations. We define it from Eq. (55) by applying the Markoffian approximation to $\zeta(t)$. This means putting the Laplace variable equal to zero in the right hand side of Eq (55), and yields

$$\tilde{\zeta}(0) = \frac{1}{\int_0^\infty \frac{E(t)-E_{th}}{E(0)-E_{th}}dt} \tag{56}$$

If the evolution were totally incoherent (exponential time-dependence), there would be no oscillations and this effective rate would equal the incoherent rate $\kappa\left(1 - e^{-\beta\hbar\Omega}\right)$. But if there are oscillations due to coherence, Eq. (56) would take them into account as they would enter the effective rate through the integration of the oscillations in the denominator of its right hand side. Eq. (56) is a prescription that can be used in this fashion on experimental observations of the energy time dependence. An interesting result emerges when we use it on the numerical solutions we have obtained above. Using the microscopic memories derived in Eqs. (19), the behavior of the Markoffian rate $\tilde{\zeta}(0)$ is plotted with respect to temperature in Fig. 7 for the strong interaction case as compared to the incoherent result of Montroll and Shuler [11]. The plot shows *multiple oscillations* with increasing T for the scaled effective rate in the strong-coupling (multiphonon) case, while exhibiting a simple and expected monotonic decay with T in the weak-coupling (single-phonon) case. By contrast, the original incoherent Master equation of Ref. [11] results in no oscillations (dashed curve) as the ratio $\tilde{\zeta}_T(0)/\tilde{\zeta}_{T=0}(0)$ in the Montroll–Shuler curve is simply $1 - e^{-\hbar\Omega/k_BT}$, with the Montroll–Shuler rate κ being equivalent to the T-independent term $\tilde{\zeta}_{T=0}(0)$. An overall nonmonotonic T dependence exists in the strong interaction regime, where the increasing or decreasing behavior is determined by the T interval in which observations are made.

5.2. The half-Markoffian approximation: developing an interpolation formula

In this section, on the basis of the *half-Markoffian* approximation discussed in Refs. [34,41], we develop a useful interpolation formula to describe the time evolution of the energy. It is found to be exact at very short and very long times, and to provide an approximate description at intermediate times. The half-Markoffian approximation is defined by taking an expression which is a convolution of two functions and approximating it by a convolutionless expression as

$$\int_0^t ds f(t-s)g(s) \approx g(t)\int_0^t ds f(s). \tag{57}$$

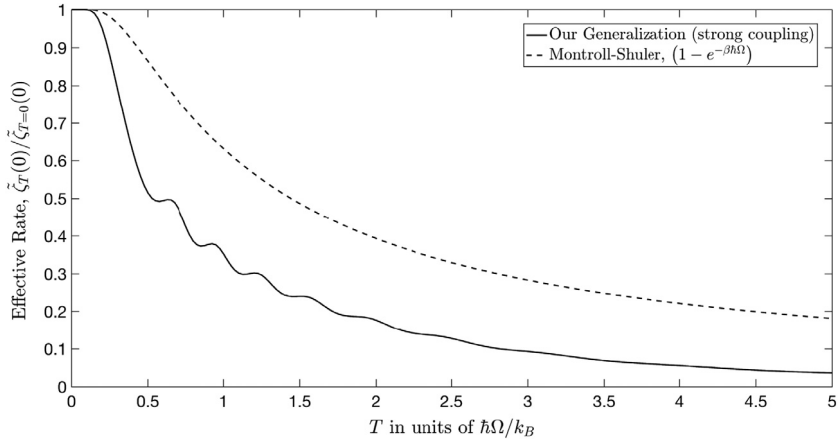

Fig. 7. Multiple oscillations (solid line) in the *temperature* dependence of the normalized effective rate of change of the energy, $\tilde{\zeta}_T(0)/\tilde{\zeta}_{T=0}(0)$ (see text) for the strong-coupling case. Parameter values are $g = 2$, $\omega_0 = \Omega$, and $\alpha/\Omega = 0.01$. For comparison, we display the same rate as calculated from the Montroll–Shuler analysis in Ref. [11] which shows no oscillations and is, indeed, $1 - e^{-\hbar\Omega/k_BT}$.

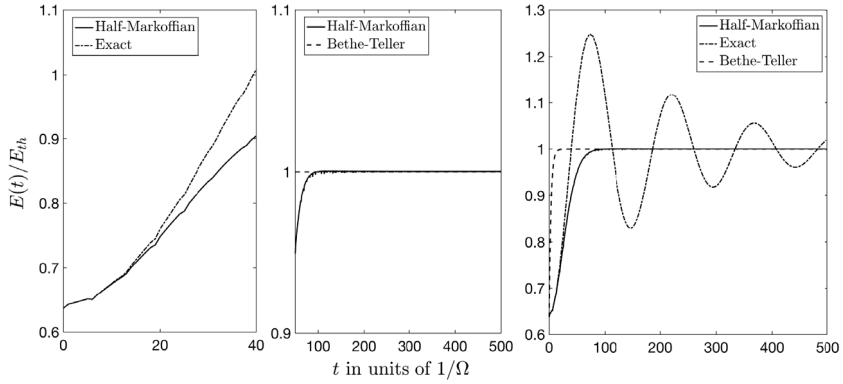

Fig. 8. Interpolation formula developed as Eq. (60) on the basis of the half-Markoffian approximation (see text) showing excellent agreement with the exact result at extreme (both short and long) times but considerable departures at intermediate times. The energy, scaled to its thermal value, is plotted for very low T for $g = 2$, $\omega_0 = \Omega + \alpha/2$, and $\alpha/\Omega = 0.02$. The kinks visible at short times (left panel) and equilibration to the steady-state result of the energy (middle panel) are faithfully reproduced by our interpolation formula. The full evolution over the three regimes of time are depicted in the right panel.

We begin by converting Eq. (44) to the integro-differential equation

$$\frac{dE(t)}{dt} + \int_0^t dt'\,\kappa\phi_D(t-t')E(t') = E_{th}\tanh\left(\frac{\beta\hbar\Omega}{2}\right)\int_0^t dt'\,\kappa\phi_S(t'), \tag{58}$$

and simplifying it further to the form

$$\frac{dE(t)}{dt} + \int_0^t dt'\,\kappa\phi_D(t-t')E(t') = \frac{\hbar\Omega}{2}\int_0^t dt'\,\kappa\phi_S(t'). \tag{59}$$

Eq. (57) is applied to the second term in Eq. (59) to yield

$$E(t) = \frac{\hbar\Omega}{2} + \left[E(0) - \frac{\hbar\Omega}{2}\right]e^{-\int_0^t dt'\mathcal{I}_D(t')} + \hbar\Omega\int_0^t dt'\mathcal{I}_+(t')e^{-\int_{t'}^t ds\mathcal{I}_D(s)}, \tag{60}$$

where $\mathcal{I}_\nu(t) = \int_0^t dt'\kappa\phi_\nu(t')$.

The exponential decay of the second term of the energy in Eq. (60) which is dependent on the difference in the memories, $\kappa\phi_D(t)$, parallels the inherent exponential decay of $\eta(t)$ in Eq. (44), starting from a finite value and decaying to zero over time. The first term describes the zero-temperature result for the energy in the steady state, which, when combined with the third term, reveals a T dependence, which in the long time limit reveals the steady-state value of the energy E_{th}. When the Markoffian approximation is applied and $\mathcal{I}_\nu(t\to\infty) = \kappa\left(1 \pm e^{-\beta\hbar\Omega}\right)$, the '+' corresponding to $\nu = S$ and the '−' to

$\nu = D$, the incoherent Montroll–Shuler [11] or Bethe–Teller [42] result is obtained:

$$E(t) = E(0)e^{-\kappa\left(1-e^{-\beta\hbar\Omega}\right)t} + E_{th}\left[1 - e^{-\kappa\left(1-e^{-\beta\hbar\Omega}\right)t}\right]. \tag{61}$$

Substitution of Eqs. (19b) and (47) into Eq. (60) shows that, indeed, the kinks arise from the behavior of the difference in the memories, at least at short times. Fig. 8 shows the half-Markoffian approximation in comparison to the exact and Bethe–Teller results. An excellent agreement of our interpolation formula is seen at both short and long times with the exact result, but it fails to predict the intermediate behavior accurately.

6. Concluding remarks

Our investigation of the relaxation to equilibrium of three simple quantum systems has uncovered some interesting and unexpected results when the system–reservoir interaction is strong. The analysis has employed a dressing transformation, polaronic in nature, that treats much of the strong interaction exactly and then treats the remaining (weak) interaction perturbatively [20–24,28]. The two interactions we have analyzed, which we have termed single-phonon or weak-coupling in one case and multiphonon or strong-coupling in the other, have the same system–bath interaction $\mathscr{V} = V_B a^\dagger a + u\left(a + a^\dagger\right)$. The first case is for weak V_B and vanishing u and the second for strong V_B and weak u, respectively. Whereas the final expression for the relaxation rate, Eq. (20), is essentially the same as one for the corresponding transition rate in standard polaron theory for the mobility of a quasi-particle moving among nonresonant states, the source of the interactions is quite different in the two cases. The main distinction is in the rationale for the term[3] that connects the two states. In the standard mobility problem, the rationale is the very motion of the quasi-particle from state to state. In our present relaxation case on the other hand, it arises from compatibility with the Landau–Teller ansatz [13] of a constant force exerted by the reservoir. This constant force is absent in standard polaron mobility theory. It corresponds, in the vibrational relaxation case of our paper, to a Hamiltonian term proportional to the displacement for the molecular oscillator, $a + a^\dagger$, and its formal structure is maintained for the other two systems analyzed.

Coarse-grained extensions [10,17,18] of the Zwanzig projection technique [14–16] have been used to obtain GME's in the system probabilities of occupation and solved explicitly for the evolution of system observables. An important element of the analysis is the initial state of the system. To ensure that the GME *without* an additional driving term can be written as given, *e.g.*, in Eq. (8), the initial state is taken to be an outer product of the system and the bath in the first case, but of the dressed system and the dressed bath in the second. As is standard in most treatments, if an initial driving term is present in the GME, it is assumed to decay faster than the memories [43].

One of the interesting effects we find is a nonmonotonic variation of the observable associated with each of the three systems. It is apparent in the temperature variation of the rate of change of the energy of the molecular oscillator (third system), see Figs. 5 and 7; in the temperature dependence of the steady-state value of the average velocity of the charged particle moving across the sites of a crystal under the influence of a strong electric field (second system), see Fig. 3 and in the occupation probability difference for the simple nonresonant dimer (first system), see Fig. 2. This effect is seen only for strong coupling (effectively multiphonon interactions). We have shown explicitly, see Fig. 6, that it does not arise for weak-coupling (single-phonon interactions).

A useful byproduct of the analysis is the half-Markoffian approximation that we have developed in Section 5. Derived from the integro-differential equation for the energy in Eq. (59), it predicts rather well the extreme, that is short- and long-time, relaxation behavior of the molecular oscillator, although it does not provide an accurate prescription for intermediate times. Its advantage lies in eliminating the necessity for excursions into the Laplace domain.

The peculiar temperature variation of the relaxation of the third system analyzed here (Section 5) may be related to observations reported by Fayer and collaborators [44,45]. The experimental report given a couple of decades ago, concerned $W(CO)_6$ dissolved in $CHCl_3$ and provided an explanation of an "inverted" T-dependence of relaxation on the basis of assumed properties of the liquid phonon density of the solvent. It is possible that our analysis in Fig. 7 might provide an alternate explanation on the basis of the more straight-forward polaronic features of the interaction that we have assumed here. We hope to return to a quantitative comparison of the explanations in a future publication.

Appendix. Comments on detailed balance

We have seen that multiplication by the damping factor $e^{-\alpha t}$ in Eqs. (19) is essential to avoid infinities given the fact [28,32] that linear interactions cannot broaden zero-phonon lines. However, the use of a single α for all transitions is an approximation that introduces its own inaccuracy. We have provided Fig. A.1 to make this clear. The rates described in Eqs. (20) and (21) satisfy detailed balance with their energetically upward transition counter-parts at higher T, but strict detailed balance fails for low T. The remedy lies in coarsening the description in ω-space and considering a rectangular function of narrow width α centered about each corresponding frequency ϖ along the spectrum, *i.e.*,

$$\frac{1}{\pi}\frac{\alpha}{\alpha^2 + \varpi^2} \approx \frac{1}{\alpha}\mathrm{rect}\left(\frac{\varpi}{\alpha}\right) = \frac{1}{\alpha}\left[\Theta\left(\varpi + \frac{\alpha}{2}\right) - \Theta\left(\varpi - \frac{\alpha}{2}\right)\right]. \tag{A.1}$$

[3] The term is the product of $a + a^\dagger$ with, respectively, V_B for the weak-coupling case and u for the strong-coupling case (see Section 2).

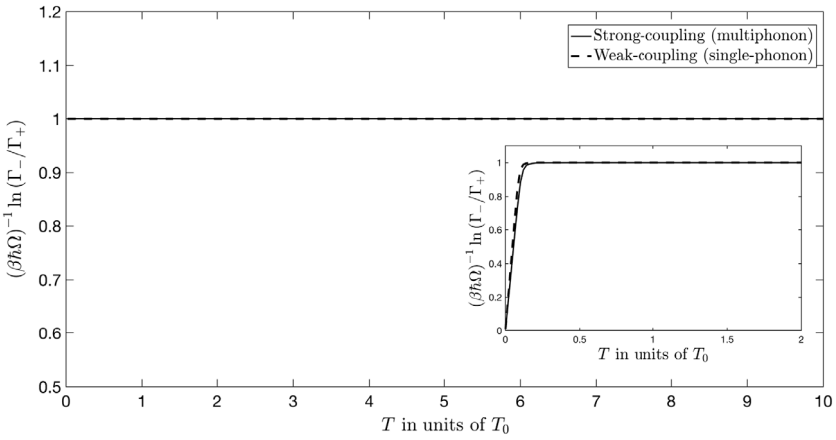

Fig. A.1. Detailed balance of the transition rates associated with each interaction regime with respect to temperature T in units of $T_0 = \hbar\omega_0/k_B$. The system is a harmonic oscillator of characteristic frequency Ω in strong ($g = 2$) and weak ($g = 0.02$) interaction with optical phonons of peak frequency $\omega_0 = \Omega$ and narrow dispersion $\alpha/\Omega = 0.01$. The conservation of detailed balance for all T is observed for the case in which the rates are described by rectangular functions (main) while strict agreement with detailed balance is observed to fail at low T, but not too dramatically, for the case in which α is introduced via Lorentzians (inset). The failure is represented by the non-coincidence of the solid and dashed lines in the inset.

The corresponding rates of Eqs. (20) and (21) may be written in terms of rectangular functions as

$$\Gamma = 2\pi \frac{u^2}{\hbar^2\alpha} e^{-g^2 \coth\left(\frac{\beta\hbar\omega_0}{2}\right)} \sum_{\ell=-\infty}^{\infty} I_\ell \left[2g^2 n\left(\omega_0\right)\right] \sum_{k=0}^{\infty} \frac{g^{2k}}{k!} \mathrm{rect}\left(\frac{(k+\ell)\omega_0 - \Omega}{\alpha}\right) \tag{A.2}$$

in the multiphonon (strong-coupling) interaction case, and

$$\Gamma = 2\pi g^2 \frac{\omega_0^2}{\alpha} \left\{ \left[n\left(\omega_0\right) + 1\right] \mathrm{rect}\left(\frac{\omega_0 - \Omega}{\alpha}\right) + n\left(\omega_0\right) \mathrm{rect}\left(\frac{\omega_0 + \Omega}{\alpha}\right) \right\} \tag{A.3}$$

in the single-phonon (weak-coupling) case, respectively. With the forms of the rates in Eqs. (A.2) and (A.3) detailed balance between the energetically upward and downward transition rates is restored (see Fig. A.1). See the narrow *peaks* (or tabletops) and sharp drop-off of the rectangular functions.

References

[1] E.G.D. Cohen, Fundamental Problems in Statistical Mechanics, North-Holland Amsterdam, Interscience Publishers, 1962.
[2] Ilya Prigogine, Non-Equilibrium Statistical Mechanics, Dover Books on Physics, 2017.
[3] Ryogo Kubo, Morikazu Toda, Natsuki Hashitsume, Statistical Physics II: Nonequilibrium Statistical Mechanics, Springer, 1998.
[4] Constantino Tsallis, Introduction to Nonextensive Statistical Mechanics, Springer, 2009.
[5] Carolyn M. Van Vliet, Equilibrium and Non-Equilibrium Statistical Mechanics, World Scientific, 2008.
[6] M. Tiwari, V.M. Kenkre, Eur. Phys. J. B 87 (2014) 4.
[7] C.A. Moyer, J. Phys. C 6 (1973) 1461.
[8] D. Emin, C.F. Hart, Phys. Rev. B 36 (1987) 2530.
[9] Charles Kittel, Quantum Theory of Solids Ed. 2, John Wiley & Sons, 1987.
[10] V.M. Kenkre, M. Chase, Internat. J. Modern Phys. B 31 (2017).
[11] E. Montroll, K. Shuler, J. Chem. Phys. 26 (1957) 3.
[12] D.W. Oxtoby, Annu. Rev. Phys. Chem. 32 (1981) 77.
[13] L. Landau, E. Teller, Phys. Z. Sow. 10 (1936) 34.
[14] R. Zwanzig, in: W.E. Brittin, B.W. Downs, J. Downs (Eds.), Lectures in Theoretical Physics, vol. 3, Interscience, New York, 1961.
[15] R. Zwanzig, Physica 30 (1964) 1109.
[16] R. Zwanzig, in: P.H.E. Meijer (Ed.), Quantum Statistical Mechanics, Gordon and Breach, New York, 1966, p. 139.
[17] V.M. Kenkre, in: U. Landman (Ed.), Statistical Mechanics and Statistical Methods in Theory and Application, Plenum, New York, 1977, p. 441.
[18] V.M. Kenkre, R.S. Knox, Phys. Rev. B 9 (1974) 5279.
[19] M. Chase, Memory Effects in Brownian Motion, Random Walks under Confining Potentials, and Relaxation of Quantum Systems (Ph.D. thesis), University of New Mexico, 2016.
[20] M.K. Grover, R. Silbey, J. Chem. Phys. 4 (1970) 2099.
[21] S. Rackovsky, R. Silbey, Mol. Phys. 25 (1973) 61.
[22] R.W. Munn, R. Silbey, J. Chem. Phys. 4 (1980) 2763.
[23] Abraham Nitzan, Chemical Dynamics in Condensed Phases: Relaxation, Transfer and Reactions in Condensed Molecular Systems, Oxford University Press, 2006.
[24] Gerald D. Mahan, Many-Particle Physics. Physics of Solids and Liquids, Plenum Publishers, 2000.
[25] A. Laubereau, W. Kaiser, Rev. Modern Phys. 50 (1978) 605.
[26] S.H. Lin, H. Eyring, Annu. Rev. Phys. Chem. 25 (1974) 39.

[27] V.M. Kenkre, A. Tokmakoff, M.D. Fayer, J. Chem. Phys. 101 (1994) 10618.
[28] V.M. Kenkre, Phys. Rev. B12 (1975) 2150.
[29] V.M. Kenkre, J.D. Andersen, D.H. Dunlap, C.B. Duke, Phys. Rev. Lett. 62 (1989) 1165.
[30] A.A. Ierides, Vibrational Relaxation Theory for Systems Embedded in Microscopically Specified Reservoirs (Ph.D. thesis), University of New Mexico, 2018.
[31] V.M. Kenkre, in: V.M. Kenkre, K. Lindenberg (Eds.), Proceedings of the PASI on Modern Challenges in Statistical Mechanics: Patterns, Noise, and the Interplay of Nonlinearity and Complexity, American Institute of Physics, 2003, p. 63.
[32] David Fitchen, in: W. Beall Fowler (Ed.), Physics of Color Centers, Academic, New York, 1968.
[33] V.M. Kenkre, Phys. Lett. 65A (5) (1978) 391.
[34] V.M. Kenkre, in: G. Hoehler (Ed.), Exciton Dynamics in Molecular Crystals and Aggregates: the Master Equation Approach, in: Springer Tracts in Modern Physics, vol. 94, Springer, Berlin, 1982.
[35] M. Fayer, private communication.
[36] V.M. Kenkre, S. Raghavan, A.R. Bishop, M.I. Salkola, Phys. Rev. B 53 (1996) 9.
[37] D.H. Dunlap, V.M. Kenkre, Phys. Rev. B 37 (1988) 6622.
[38] V.M. Kenkre, J. Phys. Chem. B 104 (2000) 3960.
[39] V.M. Kenkre, S. Raghavan, J. Opt. B: Quant. Semiclass. Opt. 2 (2000) 686–693.
[40] V.M. Kenkre, L. Giuggioli, Chem. Phys. 296 (2004) 135 (special issue).
[41] V.M. Kenkre, F. Sevilla, in: T.S. Ali, K.B. Sinha (Eds.), Contributions to Mathematical Physics: A Tribute to Gerard G. Emch, Hindustani Book Agency, New Delhi, 2007, pp. 147–160.
[42] H.A. Bethe, E. Teller, Ballistic Research Laboratory Report X-117 (1941); see also Ref. [11].
[43] V.M. Kenkre, J. Stat. Phys. 19 (1978) 333.
[44] A. Tokmakoff, M.D. Fayer, D.D. Dlott, J. Phys. Chem. 97 (1993) 1901.
[45] A. Tokmakoff, B. Sauter, M.D. Fayer, J. Chem. Phys. 100 (1994) 9035.